Materials Research. 2023; 26:e20210619
DOI: https://doi.org/10.1590/1980-5373-MR-2021-0619

Kinetic and Viscoelastic Study of Liquid Thermoplastic Matrix Based on Methyl Methacrylate Copolymers

Daniel Consoli Silveira[a], Tiago Teixeira da Silva Braga[a], Luiza dos Santos Conejo[a,c], Antônio Carlos Ancelotti Junior[b], Michelle Leali Costa[a,c], Edson Cocchieri Botelho[a]*

[a]*Universidade Estadual Paulista, Departamento de Materiais e Tecnologia, Guaratinguetá, SP, Brasil.*
[b]*Universidade Federal de Itajubá, Instituto de Engenharia Mecânica, Itajubá, MG, Brasil.*
[c]*Instituto de Pesquisas Tecnológicas, Laboratório de Estruturas Leves, São José dos Campos, SP, Brasil.*

Received: December 15, 2021; Revised: November 20, 2022; Accepted: December 31, 2022

The industries that have polymers as an important raw material in their production, such as the construction, automotive, electrical and electronic sectors, always seek innovations to cut costs, reduce weight, easiness of processing, maximizing mechanical properties, and recyclability. In this context, this work presents the study of the kinetic parameters and viscoelastic behavior of a new thermoplastic system initially liquid. Through differential scanning calorimetry (DSC) analysis, Brookfield viscosimetry; dynamic-mechanical analysis (DMA) and mathematical modeling with consolidated and standardized methods, it was possible to evaluate the polymerization kinetics and viscoelastic behavior of the material in solutions with different concentrations. The generated equations allow the prediction of the kinetic and gelation behavior of the material reducing the need for laboratory tests to determine polymer properties. The found results showed that concentrations of benzoyl peroxide initiator with 1wt% in the methyl methacrylate (MMA) copolymer solution have the best viscoelastic and dynamic-mechanical properties with a less expensive polymerization cycle.

Keywords: *polymeric matrix, thermoplastics, poly(methyl methacrylate), polymerization, kinetic parameters, viscoelastic behavior.*

1. Introduction

According to Plastics Europe[1], the biggest demands for plastic materials are packaging (39.7%), construction sector (19.8%), automotive industry (10.1%), electrical and electronics sector (6.2%), leisure and sports (4.1%), agriculture (3.4%) and the remaining 16.7% distributed among medical equipment, technical parts used for engineering and construction of machines, in addition to furniture and accessories[1-7].

Given the many applications of polymeric materials, it is relevant to note that several properties of a polymer depend on the size of its molecule, in other words, on its molar mass (molecular weight). The same polymer can have chains with different sizes, containing a wide range of values for its molar mass. Thus, it is to be expected possibilities for the development of specific properties, meeting the specific needs of each one of its numerous applications[8,9].

For example, poly(methyl methacrylate) (PMMA), popularly known as acrylic, is a thermoplastic polymer that can be found in liquid form and used with infusion and molding techniques to obtain electro-optical copolymers with side organic chains, which alters its electrical and optical characteristics, allowing its application in liquid crystals[10].

Because of the versatility of this category of polymers, the company Arkema launched its first line of a liquid thermoplastic based on MMA monomers, Elium®, which is applicable for molding into engineering parts using the same processes used for thermoset resins with the advantage of Elium® be recyclable. According to the manufacturer, this MMA-based polymer has come to cut production costs, reduce weight on engineering parts and can be used in polymeric welding or gluing processes applied on an industrial scale[11]. The thermoplastic liquid resin used in this work presents itself as the state of the art for a new generation of materials. It has low viscosity and employability in the manufacture of engineering parts of complex shapes or not, in the automotive, aeronautics, sporting goods, mechanical components, home and construction, electronics and other sectors. The Elium® family of products comes with the main objective of replacing non-recyclable thermoset resins, such as epoxy resins, however, maintaining the necessary mechanical properties[12].

Among the different polymerization mechanisms, chain polymerization has high reactivity, with active centers leading to successive additions of a large number of monomers in a chain reaction ensuring the growth and propagation of the macromolecule. After initiation through the active center, the chain continues to grow in the propagation stage, until the end of the process is achieved, a stage in which there is a reaction that leads to the disappearance of the active center at the edge of the polymeric chain by disproportion[13]. Polymers such as PMMA, based on monomers obtained from acrylic and methacrylic acid, pass-through this polymerization

*e-mail: edson.botelho@unesp.br

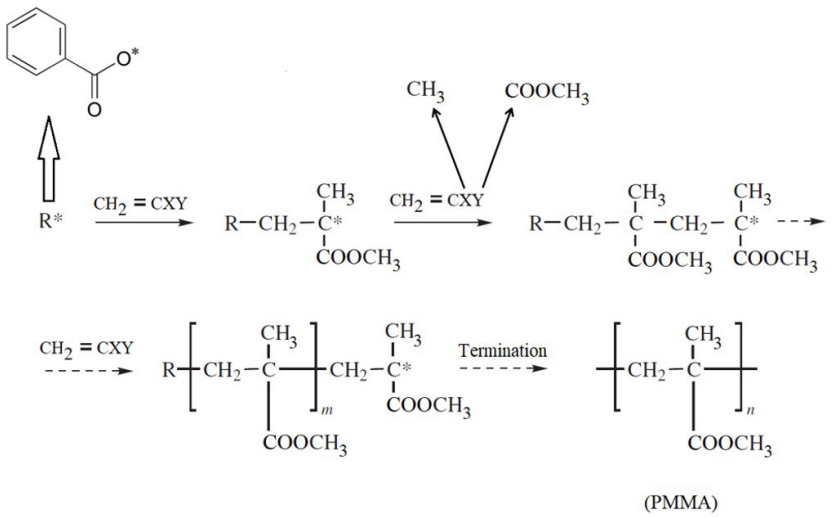

Figure 1. Free radical chain polymerization to obtain PMMA[17].

mechanism[14-16], as well as the material used in this work, Elium 591®, composed mainly of MMA vinyl monomers.

In chain polymerization via free radicals, the mechanism applied in this study, thermally unstable initiators are normally used which, when decomposed in endothermic processes, will form two active centers, that is, such as benzoyl peroxide (BzO), a thermally unstable peroxide. As can be seen in Figure 1, in chain polymerization an initiator gives rise to the active center (R*) which may be a free radical in chain polymerization via free radicals or an ion (cation or anion) in the case of ionic chain polymerization. Polymerization occurs by propagating the active center through successive additions of a large number of monomers in a chain reaction. It is characteristic of polymerization that the growth of the chain occurs only from the monomer reacting with an active center[18].

In the present work, the bulk polymerization of methacrylic esters was carried out a method widely used in the manufacture of sheets, tubes and materials for PMMA hot molding[15,16,19].

As an example of the methodology studied, Campos-Sanabria et al.[20] obtained poly (methyl methacrylate) nanocomposites with hydroxyapatite nanoparticles by polymerization via free radicals using three different concentrations of benzoyl peroxide initiator, 3, 6, and 12wt%. The results showed that the nanocomposites with the highest concentrations of BzO showed the best mechanical and tribological properties, as well as the lowest values of water absorption and pore percentage[20].

As for polymerization kinetics, there are several experimental and mathematical treatment methods for determining enthalpies, reaction rate and respective kinetic parameters, such as activation energy (E_a), Arrhenius pre-exponential factor (Z), and reaction orders (neither) of the system[21-24].

The main objective of this work is to understand the polymerization kinetic characteristics and the viscoelastic behavior of a new thermoplastic system based on copolymers of methyl methacrylate (MMA) and benzoyl peroxide (PBO) as an initiator, forming a recyclable polymer matrix.

2. Experimental

2.1. Materials

In this work, two main products were used, the thermoplastic resin Elium® 591, liquid at room temperature, and the solid initiator Luperox® 78, both supplied by the company ARKEMA Inc[25]. The thermoplastic resin used in this work is a mixture composed primarily of acrylic copolymers with a concentration between 10 and 50wt% with a specific chemical identity confidential to ARKEMA Inc. The thermoplastic resin Elium® 591 also presents in its composition 2-propenoic acid and methyl esters (CAS-No. 80-62-6) between 50 and 85wt%[25]. Type C organic peroxide, a white, granulated solid, was used as the initiator with benzoyl peroxide as its main component with a purity of 75wt% of the active component, containing 25wt% of stabilizing water with active oxygen equivalent to 5wt%[26]. Peroxide has a molecular formula $(C_6H_5CO)_2O_2$ and a molar mass of 242.23 g/mol with CAS number 94-36-0[26].

2.2. Determination of concentrations and preparation of solutions

To determine the kinetic parameters, samples of polymeric solutions were prepared with three mass concentrations of benzoyl peroxide initiator ($\tau_{I_{PBO}}$) and the thermoplastic resin based on acrylic copolymers. Therefore, the proportions between initiator and resin were weighed according to the need of each thermal analysis and the percentages in mass of BzO initiator evaluated were 0.5wt%, 1wt%, and 2wt%. Bulk polymerization of the BzO polymer systems and acrylic copolymers was accomplished mixing and homogenization of the organic initiator in the organic solution.

2.3. Differential scanning calorimetry analysis

The temperatures at the start, peak, and end of the exothermic polymerization event, in addition to the initial temperature of degradation of the polymeric systems were determined through DSC analyzes in dynamic mode.

The DSC analyzes were performed in a TA Instruments model Q20 calorimetric system, previously calibrated with indium according to ASTM E967[27] standard, for temperature, and ASTM E968[28] standard, for heat flow. All dynamic and isothermal analyzes were performed with a hermetically sealed aluminum sample holder and a controlled atmosphere of $N_{2(g)}$ with a flow rate of (50 ± 5) ml/min. The heating rate, for all dynamic experiments, was 5 °C/min and the average mass of the samples equal to 5 mg with a repetition of two analyzes for each reagent system.

The evaluations were performed according to ASTM 2070-13 standard[29]. After dynamic scans, the chosen temperatures of the isotherms were between 10-20 °C above the start of the reaction and below the peak of the exothermic event. The isothermal experiments were fulfilled by recording the heat flow as a function of time with a heating rate of 20 °C/min and the isotherm time necessary to guarantee the complete occurrence of the exothermic phenomenon. Based on the empirical results, graphs with heat flow (Y-axis) as a function of time (X-axis) were plotted. It should be noted that the evolution of the heat developed by the reaction is proportional to the conversion rate ($d\alpha/dt$) during polymerization[21,29-32].

2.4. Mathematical modeling to obtain kinetic parameters

In this work, mathematical modeling and calculations for auto-acceleration reactions were specifically applied according to the Sestak-Berggren reaction model and method B of ASTM 2070-13 standard[29].

The conversion rate of a chemical reaction ($d\alpha/dt$) is a dependent variable of the rate constant (k), which in turn is a function of the reaction temperature [k(T)], and also of a function whose independent variable is the degree of conversion of the reaction (α), α being related to the reacted fraction, according to Equation 1[24,33].

$$d\alpha/dt = k(T)\ f(\alpha) \tag{1}$$

Where:

$$\alpha = \Delta H_p/\Delta H_0 \tag{2}$$

As can be seen in Equations 1 and 2, the degree of conversion, α, is obtained by the ratio of the partial area/enthalpy of the heat flow curve, that is, ΔH_p, at a given temperature T, by the total area/enthalpy of the exothermic event, ΔH_0[21]. In the case of systems governed by autocatalytic kinetics, replacing the function f(α) by $(\alpha)^n (1-\alpha)^m$ in Equation 1, results in Equation 3, for calculating the velocity of reaction[34]. Autocatalytic reactions are those in which the formed product or intermediate functions as a catalyst in the same process, applying to autocatalysis[21,35]. The autocatalytic kinetic mechanisms are comprehensible by isothermal methods[33,36].

$$d\alpha/dt = k(T)(\alpha)^m (1-\alpha)^n \tag{3}$$

Where m and n are orders of the reaction concerning each reagent, and (m + n) is the global order of the reaction[37]. The reaction speed constant as a function of the temperature is calculated through Equation 4[22-24].

$$k(T) = Z e^{-E_a/RT} \tag{4}$$

With E_a being the activation energy (J mol^{-1}) required to initiate polymerization, T, the absolute temperature in Kelvin (K), and R, the universal gas constant (8.314 J mol^{-1} K^{-1})[22-24,29]. Z (s^{-1}) is the Arrhenius pre-exponential factor and regarding the number of collisions per unit time to achieve the reaction E_a[38].

The basis of the isothermal and autocatalytic kinetics method has a function $f(\alpha)$ equal to $(\alpha)^m (1-\alpha)^n$, according to Equation 3[29,32,34,35], which can be expressed in its logarithmic form[29,39,40]. The equation can be solved by multiple linear regression considering an equation with the form z = a + bx + cy, where $x = \ln[\alpha]$, $y = \ln[1-\alpha]$, $z = \ln[d\alpha/dt]$, $a = \ln[k(T)]$, b = m and c = n.

$$\ln[d\alpha/dt] = \ln[k(T)] + m\ln[\alpha] + n\ln[1-\alpha] \tag{5}$$

Considering the Arrhenius equation, Equation 4, for the reaction rate as a function of temperature can be expressed in its logarithmic form according to Equation 6:

$$\ln[k(T)] = \ln[Z] - \frac{E_a}{RT} \tag{6}$$

Equations 5 and 6 can be combined in their most comprehensive form according to Equation 7[41].

$$\ln[d\alpha/dt] = \ln[Z] - \frac{E_a}{RT} + m\ln[\alpha] + n\ln[1-\alpha] \tag{7}$$

Equation 7 has the form z = a + bx + cy + dw and can also be solved by multiple linear regression, where $z = \ln[d\alpha/dt]$, $a = \ln[Z]$, $b = -E_a/R$, x = 1/T, c = m, $y = \ln[\alpha]$, d = n and $w = \ln[1-\alpha]$.

In this respect, four isothermal temperatures were defined for each MMA/BzO system, for each of the three concentrations of initiator evaluated in this work resulting in 12 DSC analyzes in isothermal mode, which was performed in duplicate to guarantee the repeatability of the process, resulting in 24 tests. Isotherms were defined between the start and half of the peak reactivity of the materials. Initially, heat flow curves were prepared as a function of time for each isothermal DSC and the total reaction heat (ΔH_0) was determined, for each polymeric system, by integrating the area under the curve and limited by the baseline, drawn connecting the points immediately after the exothermic event starts and immediately before the end of the same event. For each reaction time interval, the respective reaction rates (dH/dt) in mW and the respective partial reaction heats in each time (ΔH_p) in mJ were recorded. For each fraction of the heat flow curve area, the degree of conversion (α) was determined according to Equation 2. Sequentially, the first-order derivative was determined for each degree of conversion at each time ($d\alpha/dt$). Applying Equations 6 and 7 for each polymeric system and respective BzO content, in each of the defined isotherms, and respective linear multiple regressions calculated the values of $\ln[k(T)]$ and reaction orders.

At sequence, graphs were plotted, in which the Y-axis contains values of $\ln[k(T)]$, and the X-axis values of 1/T. New linear regression techniques were performed to determine the angular coefficient (ε') and intersection point (ε") with the Y-axis for each linear regression, considering their respective standard deviations, curves fitting (R^2) and standard practices for statistical treatment of thermal analysis data according to ASTM E1970-16 standard[42]. Using the values of ε' and ε", the activation energy ($E_a = -\varepsilon' R$) and the pre-exponential collision factor ($\ln[Z] = \varepsilon''$) were determined with respective standard deviations.

2.5. Brookfield viscosimetry

The equipment used for the evaluations was the Brookfield concentric rotational viscometer model RV DV-II + Pro, connected to a Thermosel® heating chamber for tests and programmable temperature control defined with an increment of 1°C every 10 seconds. The temperature data were taken at each point immediately before a new unit increment in it, aiming at the thermal uniformity of the entire sample volume at each data collection point[43,44]. The SC4-34 spindle was applied for all analyzes dynamic, and isothermal, with a shear rate of 0.28 N and a rotation of 70 rpm[43,44]. The sample holder used for insertion into the heating chamber was the aluminum SC4-13RD and a sample volume of 9.35 mL[45]. The maximum viscosity limit of co-MMA/BzO systems during viscosimetry was set at 600 mPa.s, for all concentrations of BzO initiator and for all dynamic and isothermal analyzes. In the isothermal analysis, the spindle rotation was 70 rpm and the taking of viscosity data was performed every 3 seconds.

The polymerization kinetics can be described in terms of system viscosity raise due to the increase of the molar mass of the material during the state of gelation in the polymerization. In this sense, it can be described by the Arrhenius equation according to the chemical-rheological model presented in Equation 8[46-49].

$$\ln \mu(T,t) = \ln \mu_\infty + E_\infty / (RT) + Z_v\, t\, e^{\left[-E_{av}/(RT)\right]} \quad (8)$$

Where:
$\mu(T,t)$ = viscosity at thermodynamic temperature (T) and reaction time (t);
μ_∞ = lower viscosity in the ideal state (i.e., at an infinitely high temperature at which the resin does not undergo a polymerization process);
E_∞ = flow activation energy;
Z_v = pre-exponential factor in viscosimetry;
E_{av} = activation energy of the reaction in viscosimetry;
R = universal gas constant.

Equation 8 can be remodeled considering a fixed temperature in each isothermal viscosimetry experiment, which results in Equation 9:

$$\ln t_{gel} = \ln Z_v - E_{av}/RT \quad (9)$$

From Equation 9 it can be seen that at fixed temperatures the logarithm of the gel time ($\ln t_{gel}$) varies linearly as a function of the inverse of the temperature (1 / T). Therefore, graphs of $\ln t_{gel}$ were generated as a function of 1/T, with the activation energies of each polymeric system MMA/BzO calculated from the slope of the line ($-E_{av}/R$) and the logarithm of the pre-exponential can be obtained from the point of intersection of the line with the ordinate.

2.6. Dynamic mechanical analysis

The glass transition temperature (Tg) of polymerized samples was investigated using the DMS 6100 from SII Nanotechnology – SEIKO according to ASTM D7028[50] and E1640[51] standards. The analyses were performed at a heating rate of 2 °C/min, an oscillation amplitude of 10 µm, frequency of 1 Hz, temperature range between 30 and 200°C, nitrogen atmosphere with a flow of 100 mL/min, single cantilever mode and sample dimensions of (20 × 10 × 1.5) mm.

3. Results and Discussions

3.1. Kinetic parameters via isothermal method for reactions with auto-acceleration

In order to prove the kinetics of autocatalytic reactions in all systems, Figure 2 shows the heat flow curve as a function of time for the polymeric systems.

Figure 3 shows the dynamic DSC curves for MMA/BzO systems in different mass percentages. The analyzes had as objective obtain the values of the temperatures of the polymerization event, start temperature (T_{start}) peak temperature (T_{peak}) and end temperature (T_{end}) for the definition of the temperatures in the isothermal DSC analyzes for each polymeric system. Also, the curves allow the determination of the reaction heat, enthalpy (ΔH) through its integration.

Table 1 shows the temperatures considered for the start, peak and end of the polymerization event in dynamic DSC for each percentage of BzO initiator. Based on Table 1 and Figure 3, the thermal profile of all systems is similar, with a peak temperature of approximately 110 °C (for systems with 0.5wt% and 1.0wt% BzO) and the peak temperature around 114 °C for the 2.0wt% BzO system).

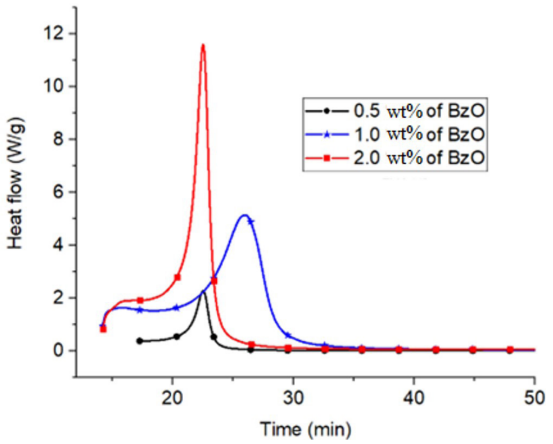

Figure 2. Heat flow vs. time curves for reactions with the autocatalytic mechanism of the polymeric systems.

Evaluating the enthalpies calculated by integrating the heat flow curves divided by sample mass as a function of temperature (Figure 3), shown in Table 1, it can observed the exothermal decreases with the increase in the content of the initiator used. The total heat released in a reactive process is dependent on the molar mass of the polymer chains formed, so greater heat released can be associated with greater efficiency in the polymerization process which in turn significantly increases in the average molar mass of the polymer chains[52]. In this sense, the enthalpies determined in this work indicate the formation of macromolecules with higher molar masses for lower levels of BzO initiator. The literature reports reaction heat during MMA polymerization equals to -54.4 kJ/mol, around -544 J g^{-1} [53]. In this work, initiator contents equal to 0.5wt% resulted in enthalpy of -548.2 J/g suggesting the total conversion of the material during its polymerization process. In general, and based on the heat released during polymerization of the MMA/1.0%BzO system (-457.3 J/g) the polymerization process of this system was also significant. For the system with 2.0wt% of BzO the heat released was -365.8 J/g. The lower enthalpy value released during this polymerization indicates a lower number of chemical bonds formed. Higher levels of an initiator are associated with a greater number of free radicals and active centers for association with monomers, propagation mechanism with greater number of polymer chains but with shorter lengths and molar masses[14,54,55] for 2wt% of BzO. Alternatively, the higher concentration of chemical initiator, consequently higher content of active centers, allowed the minimum necessary distance between a terminal carbon in a chain and an active center of the initiator causing the propagation to terminate. On the other hand, due to the greater number of chains of lower molar mass in simultaneous propagation may occur disproportionation termination in inhibitory character forming terminal unsaturation[8,16,56].

Also based on Figure 3, it is observable the presence of small secondary exothermic events. Table 2 presents the heats and temperatures related to such events and the system with 2wt% of BzO showed less value of enthalpy for such events. These secondary events may be related to secondary polymerization reactions[33,57].

Figure 4 shows the graph of percentage conversion degree (α) as a function of temperature for different %w/w of BzO initiator. The calculated values for the conversion degree of the MMA polymeric systems, for each BzO initiator content, obtained through the linear integration of the curves of the

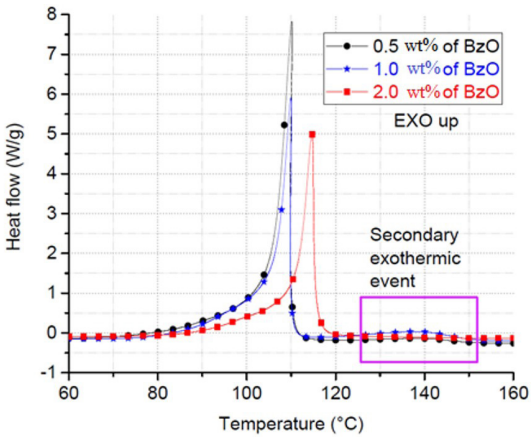

Figure 3. Dynamic DSC of MMA systems and BzO initiator in different concentrations.

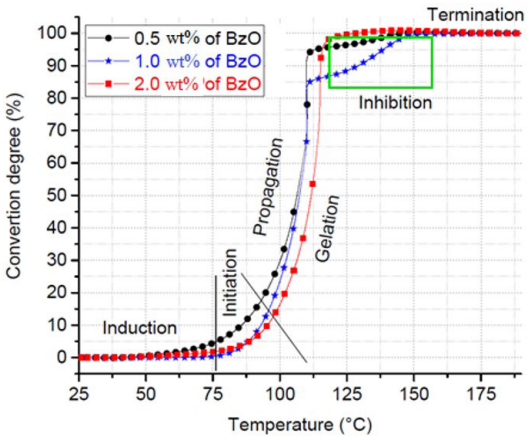

Figure 4. Percentage conversion degree (α) as a function of temperature for different wt% of BzO initiator.

Table 1. Temperatures of the polymerization event via dynamic DSC for the different mass percentages of BzO initiator.

	T_{start} (°C)	T_{peak} (°C)	T_{end} (°C)	ΔH (J/g)
0.5 wt% BzO	84.5	110.1	123.8	-548.2
1.0 wt% BzO	76.6	109.9	119.9	-457.3
2.0 wt% BzO	82.5	114.7	124.7	-365.8

Table 2. Temperatures of the second polymerization event.

	T_{start} (°C)	T_{peak} (°C)	T_{end} (°C)	ΔH (J/g)
0.5 wt% BzO	123.0	139.3	156.8	-15.88
1.0 wt% BzO	119.6	138.7	162.20	-40.80
2.0 wt% BzO	130.9	137.5	145.8	-0.14

exothermic events from Figure 3 are plotted as function of temperature in Figure 4.

In Figure 4, it is possible to observe a first plateau associated with the induction period, a period that precedes the initiation and propagation of the polymerization reactions, this period ranges from approximately 25 ° C to ~76 ° C for all polymeric systems. It is worth mentioning here that the system with 0.5wt% initiator starts before other systems, probably due to the greater mobility of the active centers in the polymeric solution[14,54,56,58]. The step of exponentially increasing of the degree of conversion in Figure 4 represents the propagation period, in which there is a gelation process with the formation of a polymeric sol-gel system of fast-growing macromolecules, significantly increasing the molar mass (gel effect). This phase ranges from ~76 °C to ~110 °C for systems with 0.5wt% and 1.0wt% of BzO and up to 115.3 °C for the system with 2 wt% of initiator. It is during this period that the system changes from a viscous liquid to an elastic gel with a relevant increase in its viscosity and shear stresses[32,36,59]. The polymerization termination phase starts at ~120 °C for the 2.0 wt% system, the first to enter this phase (vitreous effect). Systems with 0.5 wt% and 1.0 wt% BzO enter the termination phase at 150°C. The polymerization process is fully complete for all systems at ~175° C.

Also, from Figure 4, the polymeric systems achieve maximum conversion rate at temperatures of approximately 110°C (for systems with 0.5 wt% and 1.0 wt% PBO) and temperatures around 114°C (2.0 wt% PBO). Such temperatures must be properly correlated to the maximum reactivity of the polymeric systems, a fact evidenced by the peak temperatures in the dynamic DSC curves (Figure 3 and Table 1). The systems achieve 100% conversion at approximately 160 °C.

The temperatures defined for the assessments of isothermal DSC and autocatalytic modeling, following the isothermal method of ASTM E2070-13 standard[29], are 80, 110 and 120 °C for 0.5 wt% of BzO; 95, 110 and 124°C for 1.0 wt% and finally 80, 95 and 110 °C for the MMA system with 2 wt% of the initiator. Table 3 presents the kinetic parameters obtained according to ASTM E2070-13 standard[29] and method B, the values of $\overline{R^2} \geq 0.90$ indicate good adherence to the Sestak-Berggren autocatalytic model and isothermal method in determining the parameters kinetics of each MMA/BzO polymeric system. After determining the reaction orders (m and n) and ln[k(T)], the activation energy (E_a) and the collision factor (Z) of each polymeric MMA/BzO system was calculated using a new multiple linear regression from graphs of ln[k(T)] as a function of the reciprocal of absolute temperature (1/T).

Figure 5 presents the graphs of ln [k (T)] as a function of 1/T generated based on the DSC experiments in isothermal mode, Arrhenius equation expressed in its logarithmic form (Equation 6), and its resolution employing multiple linear regression. The method allows the determination of activation energies (E_a) and collision pre-exponential factor (Z) for each MMA/BzO system, with respective R^2.

Through the graphs of Figure 5, the autocatalytic polymeric system with 1 wt% of BzO initiator presents the best linear curve adjustment to obtain the activation energy parameters (E_a) and collision factor (Z), with R^2 equals to 0.95. On the other hand, the system with 0.5 wt% presented the lowest R^2 value, equal to 0.79. The linear regression determines an equation that reduces the distance between the data points and the fitted line, a R^2 value equal to 0.95 for the system with 1 wt% of BzO shows a good linear relationship between ln[k(T)] and the reciprocal of the absolute temperature (1/T). In this sense, indicating that method B for isothermal DSC experiments and Sestak-Berggren autocatalytic reactions of, according to ASTM E2070-13 standard[29], was reasonably applied in this work, enabling the determination of the polymerization kinetics and respective parameters for the MMA system and BzO initiator, mainly for the system with 1 wt% of initiator. Probably, the low adjustment of R for the other concentrations of BzO indicates that the autocatalytic mechanism was not as effective to describe its polymerization kinetics in the studied isotherms or to be necessary to perform a larger number of DSC experiments in isothermal mode, obtaining a greater number of input data and thus enabling a better linear fit.

The dependence of the conversion rate, during polymerization via free radicals, concerning the kinetic parameters, according to the Sestak-Berggren model, for each system of methyl methacrylate copolymers and benzoyl peroxide initiator are presented in Equations 10, 11 and 12 (based on the Equation 7).

For MMA/0.5 wt% of BzO:

$$\ln\left(d\alpha / dt\right) = 18.24 - 34.52 / RT + 0.54 \ln\left[\alpha\right] + 0.64 \ln\left[1 - \alpha\right] \quad (10)$$

For MMA/1.0 wt% of BzO:

$$\ln\left(d\alpha / dt\right) = 35.15 - 88.85 / RT + 0.90 \ln\left[\alpha\right] + 0.61 \ln\left[1 - \alpha\right] \quad (11)$$

For MMA/2.0 wt% of BzO:

$$\ln\left(d\alpha / dt\right) = 25.76 - 60.24 / RT + 0.22 \ln\left[\alpha\right] + 0.67 \ln\left[1 - \alpha\right] \quad (12)$$

The polymeric system MMA/0.5 wt% of BzO presented the lowest activation energy among all, E_a equals to

Table 3. Kinetic parameters for polymerization via Sestak-Berggren autocatalytic reactions for each polymeric system in different wt% of BzO initiator.

wt% BzO	Kinetic parameters						
	Ln Z (s^{-1})	Ea (kJ mol^{-1})	$\bar{m}$	$\bar{n}$	Global order	ΔH (J/g)	$\overline{R^2}$
0.5	18.24 ± 5.68	34.54 ± 17.7	0.54 ± 0.008	0.64 ± 0.003	1.18	-548.2*	0.94
1.0	35.15 ± 6.27	88.85 ± 19.9	0.90 ± 0.030	0.61 ± 0.004	1.51	-457.3*	0.92
2.0	25.76 ± 5.41	60.24 ± 16.6	0.22 ± 0.011	0.67 ± 0.004	0.89	-365.8*	0.90

*Enthalpies (ΔH) from the dynamic DSC experiments.

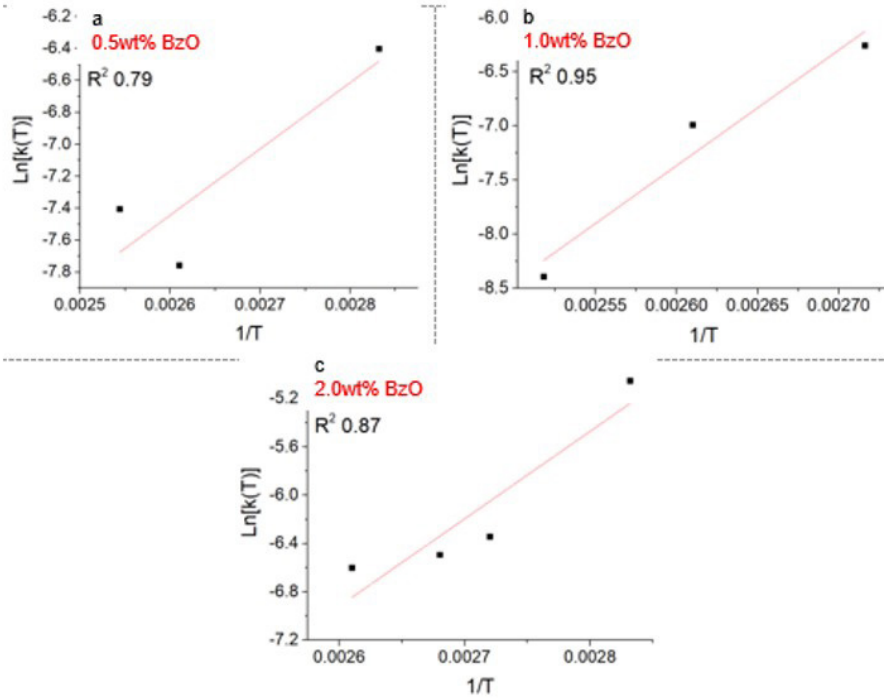

Figure 5. Graphs ln [k(T)] vs. 1/T based on isothermal DSC experiments and Arrhenius equation: (a) 0.5wt% BzO; (b) 1.0 wt% BzO and (c) 2.0 wt% BzO.

34.52 kJ/mol. In fact, this system is the one that remains in levels of lower viscosity at relatively high temperatures has a gel temperature (T_{gel}) equals to 89.1 °C, and has viscosities below 100 mPa.s at temperatures below 79.2 °C, as shown in Figure 6. The low viscosity of this system allows a high diffusion of the active centers between the monomers, greater miscegenation between the reagents, consequently facilitating the beginning of the reaction process. Figure 4 contributes to such inference, observing the conversion degree curves, the system with 0.5 wt% of BzO leaves the induction and enters the initiation phase before the other polymeric systems, presenting relatively higher conversion at lower initial temperatures (α = 4.5% at 75 °C). The MMA/1.0 wt% BzO system has the highest activation energy (E_a = 88.85 kJ mol^{-1}), therefore with the greatest energy barrier to start the conversion process justifying its modest α = 0.33% at 75 °C. According to Matyjaszewski and Davis[60] the activation energies for polymerization reactions of MMA monomers via thermally unstable initiators, such as BzO, are close to 80 kJ mol^{-1}.

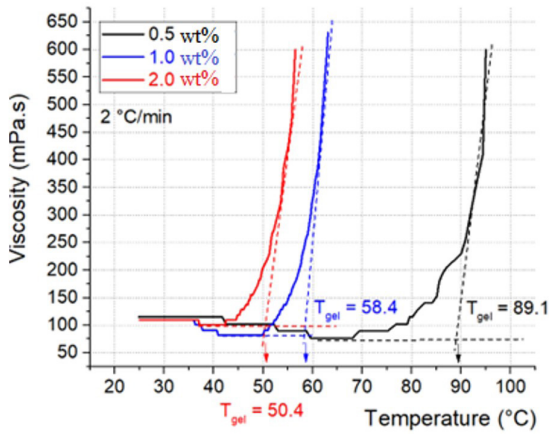

Figure 6. Brookfield dynamic viscosimetry for polymeric MMA/BzO systems.

Table 3 above also shows the values of Ln Z (s^{-1}) for the MMA/BzO reaction media, with Z being the pre-exponential factor and relates to the average frequency of collisions between the reagents every second. It is from these collisions that the reagents obtain the necessary and sufficient energy (Energy ≥ Ea) to start the process of their conversion into the products of the polymerization process. In this work, satisfactory values were obtained for the pre-exponential factor (Z), being $Z_{0.5wt\%BzO}$ = 8.4 x 10^7 s^{-1}; $Z_{1.0wt\%BzO}$ = 1.8 x 10^{15} s^{-1}; $Z_{2.0wt\%BzO}$ = 1.5 x 10^{11} s^{-1}. It is again evident the importance of the propagation step in the system with 1.0 wt% of BzO, the one with the largest pre-exponential factor. Despite its modest initial conversion rate, the last system to effectively exit induction and enter the initiation phase (mainly due to its high E_a), the same system undergoes major reaction progress during the propagation and gelation phase. Reaching a degree of conversion higher than 80% (~110 ° C) before the other polymeric systems growth is mainly related to its high Z factor[15,60].

Table 4 shows the individual reaction orders for each system and respective standard deviations for each multiple linear regression, based on the performed DSC in isothermal

Table 4. Reaction orders and respective standard deviations for each DSC experiment in isothermal mode, including to the respective R^2.

wt% PBO	$T_{isotherm}$ (°C)	M	N	R^2
0.5	80	0.514 ± 0.007	0.750 ± 0.005	0.97
	110	0.214 ± 0.004	0.591 ± 0.001	0.97
	120	0.885 ± 0.012	0.583 ± 0.002	0.89
1.0	95	0.299 ± 0.012	0.794 ± 0.006	0.85
	110	1.082 ± 0.025	0.605 ± 0.004	0.93
	124	1.303 ± 0.051	0.430 ± 0.002	0.99
2.0	80	0.303 ± 0.007	0.713 ± 0.004	0.90
	95	0.252 ± 0.017	0.661 ± 0.005	0.89
	110	0.112 ± 0.008	0.626 ± 0.003	0.91

mode and, respectively, R^2. From the analysis of Table 4, it is confirmed that all polymeric systems can be described by autocatalytic reaction mechanisms, but for the formulation MMA/0.5 wt% of BzO the order n is predominant up to 110 °C, so that its polymerization is much more driven by the consumption of reagents, concentration of monomers and initiator, than by autocatalysis due to the formation of intermediates[15,47,60]. Similarly, the polymeric system with 1.0 wt% of BzO initiator shows similar behavior for isotherm of 95°C, but for temperatures of 110 and 124°C the autocatalytic behavior prevails, and the formation of intermediaries in the process effectively self-accelerate or self-catalyze, the polymerization process. For the polymer system with MMA copolymer and BzO initiator at a concentration of 2 wt% prevails the order n in all the temperatures evaluated, therefore, this system intrinsically depends on the consumption of monomers ([M]) and initiator ([I]) for the development of their polymerization reactions[15,47,60].

3.2. Viscoelastic and kinect parameters via brookfield viscosimetry

From the dynamic viscosimetry (Figure 6) and the gelation data, the increase in the BzO concentration reduces the gel temperature (T_{gel}), being 89.1 °C for the system with 0.5 wt% of BzO and 50.4 °C for the system with 2.0%. The properties of a polymer vary asymptotically to a reference value as the molar mass of the polymer increases[61,62]. In this sense, the MMA/BzO systems reach maximum viscosities at lower temperatures with an increase in the initiator concentration.

Table 5 shows the defined isotherms for the Brookfield viscosimetry, and Figure 7 shows the Neperian logarithm of the gel time ($\ln t_{gel}$) as a function of the inverse of the absolute temperature (1/T). In this sense, the Arrhenius model, presented in Equations 8 and 9, allows obtaining the values of activation energy of the gelation process during viscosimetry shown in Table 4.

The results suggest that the higher the concentration of benzoyl peroxide initiator, the lower the energy barrier to be overcome by the system to start its gelation process, thus the MMA/2.0 wt% BzO system achieves greater reactivity faster, forming a biphasic sol-gel system before the others.

Table 5. Activation energy values for the gelation of the MMA/BzO systems in different wt% of initiator and gel time in the isotherms.

	0.5 wt% BzO	1.0 wt% BzO	2.0 wt% BzO
E_{av} (kJ mol^{-1})	44.94 ± 2.46	28.40 ± 2.18	22.43 ± 2.67
t_{gel} (min)	4.6 at 70 °C	10.3 at 50 °C	9.4 at 45 °C
	6.3 at 65 °C	11.4 at 45 °C	10.3 at 40 °C
	6.7 at 60 °C	14.6 at 40 °C	11.4 at 36 °C
	37.3 at 30 °C	20.2 at 30 °C	14.4 at 30 °C

This is also in line with the results of dynamic viscosimetry presented and as observed during the experiments. Significant increases in the viscosity values of polymeric systems are directly related to the formation of oligomers in the system, which in turn are dependent on the thermal decomposition of the BzO, thus increasing the concentration of active centers and promoting a greater union of monomeric units and their propagation[15,47,60]. Thus, an increase in the molecular mass of the system leads to loss of mobility of the polymer chains quickly for higher concentrations of BzO initiator and in higher isotherms. The increase in the BzO concentration from 0.5 wt% to 2.0 wt% led to a 50% reduction in the activation energy needed to start the gelation process. In addition, this is reflected in the gel times of each system, lower t_{gel} were determined for systems with a higher concentration of initiator for the same temperature range. As shown in Table 4 and Figure 8.

Note that in the same isotherm (30°C) the system with 0.5 wt% of BzO has a gel time of 37.3 min, while the system with 1.0% has 20.2 min and the system with 2.0% 14.4 min. Also based on Figure 8, for the same MMA/ BzO system, higher temperatures/isotherms lead to a decrease in t_{gel}. That is, both the defined isotherm and the initiator concentration are parameters of effect on the t_{gel} and reactivity of the polymer in isothermal environments of constant rotation. On the other hand, due to the faster gelation, systems with higher initiator content have a narrower range of temperatures possible for isothermal experiments.

Parabolic curve adjustments were determined for all three MMA/ BzO systems evaluated in this work, with R^2 greater than 0.98 for all. Based on mathematical modeling

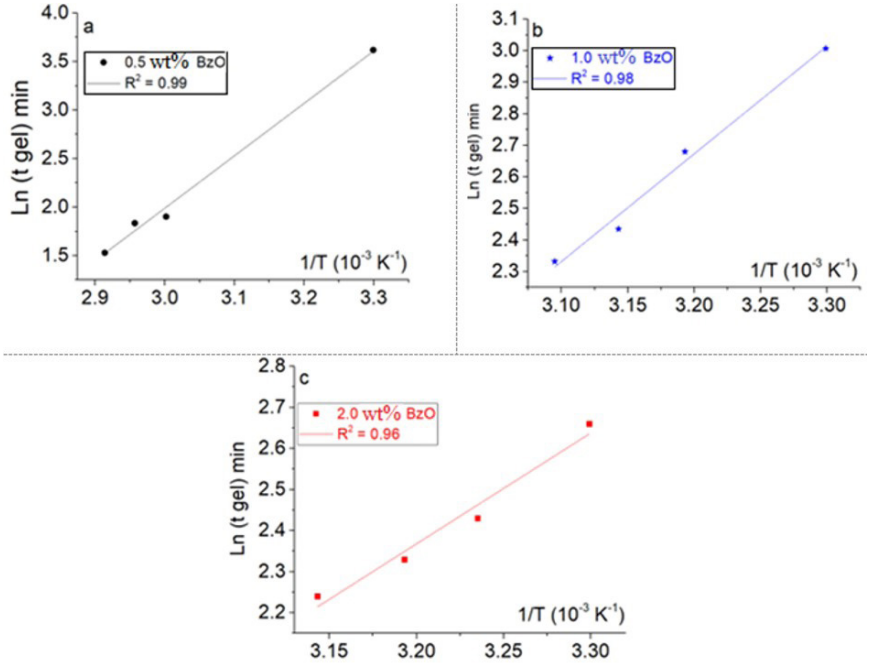

Figure 7. ln t_{gel} *vs.* 1/T graphs for each MMA/BzO system: (a) 0.5wt% BzO; (b) 1.0 wt% BzO and (c) 2.0 wt% BzO

and determined polynomial regression, the correct equation is applicable to predict the t_{gel} of each MMA/BzO system in pre-defined isotherms, according to the Equations 13, 14 and 15:

For MMA/0.5 wt% of BzO:

$$t_{gel} = 102.70 - 2.77 \; x \; T_{isotherm}^{1} + 0.02 \; x \; T_{isotherm}^{2} \quad (13)$$

For MMA/1.0 wt% of BzO:

$$t_{gel} = 50.09 - 1.29 \; x \; T_{isotherm}^{1} + 0.01 \; x \; T_{isotherm}^{2} \quad (14)$$

For MMA/2.0 wt% of BzO:

$$t_{gel} = 47.42 - 1.62 \; x \; T_{isotherm}^{1} + 0.02 \; x \; T_{isotherm}^{2} \quad (15)$$

Arrhenius plots of the type $\ln t_{gel}$ *vs.* 1/T can present points of convergence indicating temperatures in which the gelation process occurs slowly, in which the polymer is closer to a glassy state, presenting reduced mobility of their chains, consequently depreciating the speed of the process[46]. From Figure 9, three points of convergence of which the two at the edges and indicated in the graph delimit a probable region for estimating the glass transition temperature (T_g) of the polymeric MMA/BzO systems. The two points of convergence T_g of the studied material are between 326.8 K and 340.1 K (54° C ≤ T_g ≤ 67°C).

Complementary experiments of dynamic-mechanical analysis (DMA) were carried out to determine the glass transition temperature (Tg) for the MMA/BzO systems studied in this work. Table 6 presents the Tg results obtained by the peak maximum of tan δ for the MMA/BzO systems. Considering the processing parameters applied to MMA/BzO systems, specifically in this work, it is observed that

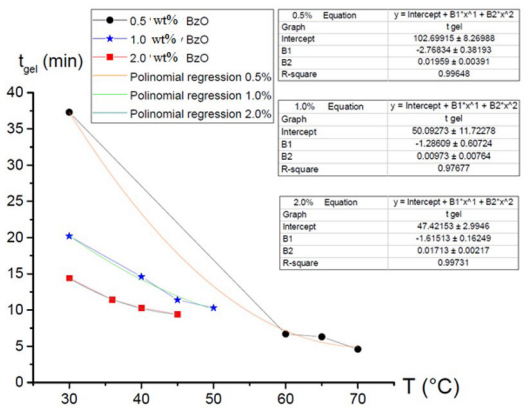

Figure 8. Gel time for each MMA/BzO polymeric system during isothermal viscometry and respective regressions.

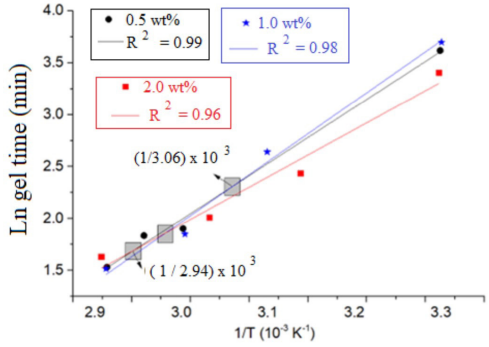

Figure 9. Arrhenius graph for all MMA/BzO systems and congruence points.

Table 6. T_g values obtained from peak of tan delta in the DMA curves for PMMA systems prepared with distinct wt% of BzO.

	Frequency (Hz)	T_g (°C)		
		0.5 wt% PBO	1.0 wt% PBO	2.0 wt% PBO
Tan δ	1	47.6	52.1	61.5

the average Tg of the polymer with 0.5wt% BzO is equal to 47.6°C and the increase in the concentration of initiator leads to an increase in Tg average, being 52.1°C and 61.5°C for 1.0 wt% and 2.0 wt% of BzO, respectively. This one behavior confirms that the increase in BzO hinders the mobility of the polymer chain, requiring more energy to occur the internal movement of the polymer, increasing, therefore, the working temperature of the same. Also, for processing parameters applied in the materials of this study, the glass transition temperatures for the polymeric systems with 1.0 wt% and 2.0 wt% of BzO, determined via DMA, show good correlation with the Tg range obtained based on Figure 9 and the Arrhenius graphs via viscometers Brookfield (54°C ≤ Tg ≤ 67°C). Thus, the values obtained indicating success in the mathematical correlation and viscoelastic modeling between Brookfield viscosimetry and dynamic-mechanical analysis.

4. Conclusions

Copolymers based on acrylic monomers were produced employing bulk polymerization with the variation of the content of benzoyl peroxide (BzO) thermal unstable initiator. The three polymeric systems studied (0.5 wt%, 1 wt%, and 2 wt% of BzO) indicate good adherence to the autocatalytic mathematical model of Sestak-Berggren in the determination of kinetic parameters. The polymeric system MMA/0.5 wt% of BzO showed the lowest activation energy among all calculated, E_a equals to 34.52 kJ mol^{-1}, in fact, this MMA/BzO system is the one that remains in levels of lower viscosity at relatively high temperatures. The same system has a gel temperature (T_{gel}) equals to 89.1 °C and has viscosities below 100 mPa.s at temperatures below 79.2 °C. On the other hand, the MMA/1.0 wt% BzO system has the highest activation energy (E_a = 88.85 kJ mol^{-1}), therefore with a greater energy barrier to start the conversion process (α = 0.31% at 75 °C). However, the importance of the propagation step in the system with 1.0 wt% of BzO is evident, it presented the largest pre-exponential factor ($Z_{1.0wt\%BzO}$ = 1.8 x 10^{15} s^{-1}). Despite its modest initial conversion rate, this being the last system to effectively exit induction and enter the initiation phase (mainly due to its high E_a), the same system undergoes major reaction progress during the propagation and gelation phase. Reaching a degree of conversion above 80% (~110 °C) before the other polymeric systems growth mainly related to its high Z factor.

Studies of dynamic and isothermal Brookfield viscosimetry and the application of the Arrhenius model allowed obtaining the activation energy values of the gelation processes during viscosimetry. Lower activation energies were observed for higher levels of BzO initiator with 44.94 kJ mol^{-1} for 0.5 wt% of initiator; 28.40 kJ mol^{-1} for 1.0 wt%, and 22.43 for 2.0 wt%. What in turn is reflected in the gel times of each system, lower t_{gel} were observed for systems with a higher concentration of initiator for the same temperature range. Mathematical models were effectively created to describe the polynomial influence of the isothermal temperature on the gel times of the systems, parabolic curve adjustments were determined for all three MMA/BzO systems evaluated with R^2 greater than 0.98 for all.

The glass transition temperatures determined via dynamic-mechanical analysis for the polymeric systems show a good correlation with the T_g range obtained based on the Arrhenius graphs via Brookfield viscosimetry, indicating success in the mathematical correlation and viscoelastic modeling between Brookfield viscosimetry and DMA. The relatively low T_g values obtained via DMA indicate the importance of controlling the stereochemistry (tacticity) of PMMA, suggesting that anionic polymerization processes may be preferable in obtaining PMMA with the mixture of copolymers used in this work allowing the formation of syndiotactic microstructure.

5. Acknowledgments

The authors are grateful for the financial support given by the Brazilian Funding Institutions: São Paulo Foundation Research (FAPESP), National Council for Scientific and Technological Development (CNPq) (140852/2018-2, 306576/2020-1 and 304876/2020-8) and this study was financed in part by the Coordenação de Aperfeiçoamento de Pessoal de Nível Superior – Brazil (CAPES) – Finance Code 001 and ARKEMA for the supply of Elium® 591.

6. References

1. Plastics Europe: Association of Plastics Manufactures. Plastics: the Facts 2018: an analysis of Europe plastics production, demand and waste data [Internet]. Brussels; 2018 [cited 2021 Nov 20]. Available from: https://www.plasticseurope.org/application/files/6315/4510/9658/Plastics_the_facts_2018_AF_web.pdf
2. Vasconcelos GC, Mazur RG, Ribeiro B, Botelho EC, Costa ML. Evaluation of decomposition kinetics of poly (ether-ether-ketone) by thermogravimetric analysis. Mater Res. 2014;17(1):227-35. http://dx.doi.org/10.1590/S1516-14392013005000202.
3. Bourlegat LR, Damato CA, Silva DF, Botelho EC, Pardini LC. Processing and mechanical characterization of titanium-graphite hybrid laminates. J Reinf Plast Compos. 2010;29(22):3392-400. http://dx.doi.org/10.1177/0731684410377541.
4. Botelho EC, Rezende MC, Pardini LC. Hygrothermal effects evaluation using the Iosipescu shear test for glare laminates. J Braz Soc Mech Sci Eng. 2008;30(3):213-20.
5. Botelho EC, Almeida RS, Pardini LC, Rezende MC. Influence of hygrothermal conditioning on the elastic properties of carall laminates. Appl Compos Mater. 2007;14(3):209-22. http://dx.doi.org/10.1007/s10443-007-9041-3.
6. Botelho EC, Nogueira CL, Rezende MC. Monitoring of nylon 6,6/carbon fiber composites processing by X-ray diffraction

and thermal analyses. J Appl Polym Sci. 2002;86(12):3114-9. http://dx.doi.org/10.1002/app.11335.
7. Almeida RS, Damato CA, Botelho EC, Pardini LC, Rezende MC. Effect of surface treatment on fatigue behavior of metal/carbon fiber laminates. J Mater Sci. 2008;43(9):3173-9. http://dx.doi.org/10.1007/s10853-008-2528-y.
8. Wypych G. Handbook of polymers. Toronto: Chemtec; 2012. http://dx.doi.org/10.1016/C2011-0-04631-8.
9. Botelho EC, Scherbakoff N, Rezende MC. Study of polyamide 6/6 synthesis carried out by interfacial polymerization on carbon fiber. Polym Int. 2002;51(11):1261-7. http://dx.doi.org/10.1002/pi.1064.
10. Najjar R, Bigdeli E. Synthesis of novel core-shells of PMMA with coumarin based liquid crystalline side chains and PMMA shell as electro-optical materials. Eur Polym J. 2018;104:136-46. http://dx.doi.org/10.1016/j.eurpolymj.2018.05.012.
11. Reinforced Plastics. Composite developments drive auto industry forward. Reinf Plast. 2014;58(3):22-5. http://dx.doi.org/10.1016/S0034-3617(14)70135-3.
12. Arkema. Arkema Group at a glance [Internet]. 2019[cited 2021 Nov 20]. Available from: https://www.arkema.com/en/arkema-group/profile
13. Mohapatra H, Kleiman M, Esser-Kahn AP. Mechanically controlled radical polymerization initiated by ultrasound. Nat Chem. 2017;9(2):135-9. http://dx.doi.org/10.1038/nchem.2633.
14. Salimgareeva VM, Kolesov SV. Plastic scintillators based on polymethyl methacrylate: a review. Instrum Exp Tech. 2005;48(3):273-83. http://dx.doi.org/10.1007/s10786-005-0052-8.
15. Kricheldorf HR, Nuyken O, Swift G. Handbook of polymer synthesis. 1st ed. New York: Marcel Dekker; 2005. 965 p.
16. Stuart B. Polymer analysis. 1st ed. Chichester: John Wiley & Sons; 2002. 279 p.
17. Odian G. Principles of polymerization. 4th ed. New York: Wiley-Interscience; 2004. 812 p.. http://dx.doi.org/10.1002/047147875X.
18. Yong X, Kuksenok O, Balazs AC. Modeling free radical polymerization using dissipative particle dynamics. Polymer. 2015;72:217-25. http://dx.doi.org/10.1016/j.polymer.2015.01.052.
19. Akae Y, Sogawa H, Takata T. Cyclodextrin-based [3]rotaxane-crosslinked fluorescent polymer: synthesis and de-crosslinking using size complementarity. Angew Chem Int Ed Engl. 2018;130(45):14832. http://dx.doi.org/10.1002/ange.201809171. PMid:30239079.
20. Campos-Sanabria V, Hernández-Sierra MT, Bravo-Sanchéz M, Aguilera-Camacho LD, García-Miranda JS, Moreno KJ. Tribological and mechanical characterization of PMMA/HAp nanocomposites obtained by free- radical polymerization. MRS Adv. 2018;3(63):3763-8. http://dx.doi.org/10.1557/adv.2018.622.
21. ASTM: American Society for Testing and Materials. ASTM E2041-13: standard test method for estimating kinect parameters by differential scanning calorimeter using the borchardt and daniels method. West Conshohocken: ASTM; 2013.
22. Jankovic B. Kinetic and reactivity distribution behaviors during curing process of carbon/epoxy composite with thermoplastic interface coatings (T800/3900-2 prepreg) under the nonisothermal conditions. Polym Compos. 2016;39(1):201-20. http://dx.doi.org/10.1002/pc.23920.
23. Rezende MC, Costa ML, Botelho EC. Structural composites: tecnologia e prática. 1ª ed. São Paulo: ArtLiber; 2011. 396 p.
24. Trache D, Abdelaziz A, Siouani B. A simple and linear isoconversional method to determine the pre-exponential factors and the mathematical reaction mechanism functions. J Therm Anal Calorim. 2017;128(1):335-48. http://dx.doi.org/10.1007/s10973-016-5962-0.
25. Arkema. ELIUM® material safety data sheet [Internet]. 2014 [cited 2021 Nov 20]. Available from: https://www.b2bcomposites.com/msds/atofina/626572
26. Sigma-Aldrich. Security information of Luperox® A75, Benzoyl peroxide [Internet]. 2021 [cited 2021 Nov 20]. Available from: https://www.sigmaaldrich.com
27. ASTM: American Society for Testing and Materials. ASTM E967-18: standard test method for temperature calibration of differential scanning calorimeters and differential thermal analyzers. West Conshohocken: ASTM; 2018.
28. ASTM: American Society for Testing and Materials. ASTM E968-02: standard practice for heat flow calibration of differential scanning calorimeters. West Conshohocken: ASTM; 2014.
29. ASTM: American Society for Testing and Materials. ASTM E2070-13: standard test method for kinetic parameters by differential scanning calorimetry using isothermal methods. West Conshohocken: ASTM; 2018.
30. ASTM: American Society for Testing and Materials. ASTM E2890-12: standard test method for kinetic parameters for thermally unstable materials by differential scanning calorimetry using the kissinger method. West Conshohocken: ASTM; 2013.
31. Qiu L, Wang K, Zhu S, Lu Y, Luo G. Kinetics study of acrylic acid polymerization with a microreactor platform. Chem Eng J. 2016;284:233-9. http://dx.doi.org/10.1016/j.cej.2015.08.055.
32. Costa ML, Botelho EC, Rezende MC. Monitoring of Cure Kinetics Prepreg and Cure Cycle Modeling. J Mater Sci. 2006;41(13):4349-56. http://dx.doi.org/10.1007/s10853-006-6082-1.
33. Akay M. Introduction to polymer science and technology. 1st ed. Portugal: Bookboon; 2019.
34. Yu X, Shang Z, Zhang K. Thermally stable polybenzoxazines via tetrahydrophthalimide-functional monobenzoxazines: synthesis, characterization and thermally activated polymerization kinetics. Thermochim Acta. 2019;675:29-37. http://dx.doi.org/10.1016/j.tca.2019.03.006.
35. Mezhuev Y, Korshak YV, Shtilman MI, Pokhil SE, Strakhov IS. Kinetic features of N-ethylaniline polymerization. Russ J Gen Chem. 2015;85(6):1017-21. http://dx.doi.org/10.1134/S1070363215060213.
36. Azimi HR, Rezaei M, Majidi F. The non-isothermal degradation kinetics of St-MMA copolymers. Polym Degrad Stabil. 2014;99:240-8. http://dx.doi.org/10.1016/j.polymdegradstab.2013.10.023.
37. Ferrer N, Serra E, Sempere J, Nomen R. Non-parametric kinetic analysis of autocatalytic reactions. J Loss Prev Process Ind. 2017;49:357-66. http://dx.doi.org/10.1016/j.jlp.2017.08.001.
38. Chen C, Miao W, Zhou C, Wu H. Thermogravimetric pyrolysis kinetics of bamboo waste via Asymmetric Double Sigmoidal (Asym2sig) function deconvolution. Bioresour Technol. 2017;225:48-57. http://dx.doi.org/10.1016/j.biortech.2016.11.013. PMid:27883953.
39. Vijayan P P, Puglia D, Rastin H, Saeb MR, Shojaei B, Formela K. Cure kinetics of epoxy/MWCNTs nanocomposites: isothermal calorimetric and rheological analyses. Prog Org Coat. 2017;108:75-83. http://dx.doi.org/10.1016/j.porgcoat.2017.04.005.
40. Xiong X, Zhou L, Ren R, Liu S, Chen P. The thermal decomposition behavior and kinetics of epoxy resins cured with a novel phthalide-containing aromatic diamine. Polym Test. 2018;68:46-52. http://dx.doi.org/10.1016/j.polymertesting.2018.02.012.
41. Yang C, Wen G, Zhu X, Tang P. A multivariate linear regression method based on an improved rate equation to determine parameters of nonisothermal crystallization kinetics. Thermochim Acta. 2017;656:1-9. http://dx.doi.org/10.1016/j.tca.2017.08.005.
42. ASTM: American Society for Testing and Materials. ASTM E1970-16: standard practice for statistical treatment of thermoanalytical data. West Conshohocken: ASTM; 2013.
43. Gaefke CB, Botelho EC, Ferreira NG, Rezende MC. Effect of furfuryl alcohol addition on the cure of furfuryl alcohol resin used in the glassy carbon manufacture. J Appl Polym Sci. 2007;106(4):2274-81. http://dx.doi.org/10.1002/app.26938.

44. Oishi SS, Rezende MC, Origo FD, Damião AJ, Botelho EC. Viscosity, pH and moisture effect in the porosity of poly(furfuryl alcohol). J Appl Polym Sci. 2013;128(3):1680-6.
45. RG Strumenti. Viscometer Software RheocalcT. Italy; 2019.
46. Yang M, Zhang Z, Yuan J, Wu L, Zhao X, Guo F, et a. Fabrication of PTFE/Nomex fabric/phenolic composites using a layer-by-layer self-assembly method for trybology field application. Friction. 2020;8(2):335-42. http://dx.doi.org/10.1007/s40544-019-0260-z.
47. García-Martinez V, Gude MR, Ureña A. Understanding the curing kinetics and rheological behaviour of a new benzoxazine resin for carbono fibre composites. React Funct Polym. 2017;129:103-10. http://dx.doi.org/10.1016/j.reactfunctpolym.2017.02.005.
48. Lucio B, de la Fuente JL. Rheological cure characterization of an advanced functional polyurethane. Thermochim Acta. 2014;596:6-13. http://dx.doi.org/10.1016/j.tca.2014.09.012.
49. Zhang L, Zhang Y, Wang L, Yao Y, Wang L, Wang H, et al. Rheological and curing behaviors of high heat-resistant benzoxazine resin. Polym Test. 2018;69:214-8. http://dx.doi.org/10.1016/j.polymertesting.2018.05.018.
50. ASTM: American Society for Testing and Materials. ASTM D7028: Standard Test Method for Glass Transition Temperature (DMA Tg) of Polymer Matrix Composites by Dynamic Mechanical Analysis (DMA). West Conshohocken: ASTM; 2015.
51. ASTM: American Society for Testing and Materials. ASTM E1640: Standard Test Method for Assignment of the Glass Transition Temperature By Dynamic Mechanical Analysis. West Conshohocken: ASTM; 2018**.**
52. Meyer T, Keurentjes J. Handbook of polymer. 1st ed. Weinheim: Wiley-VCH; 2005. 1102 p.
53. Casson V, Snee T, Maschio G. Investigation of an accident in a resins manufacturing site: the role of accelerator on polymerization of methyl methacrylate. J Hazard Mater. 2014;270:45-52. http://dx.doi.org/10.1016/j.jhazmat.2014.01.038. PMid:24531369.
54. Kozak R, Matlengiewicz M. Effect of enthalpy of polar modifiers interaction with n-butyllithium on the reaction enthalpy, kinetics and chain microstructure during anionic polymerization of 1,3-butadiene. Polym Test. 2017;64:20-37. http://dx.doi.org/10.1016/j.polymertesting.2017.09.029.
55. Raponi OA, de Souza BR, Barbosa LCM, Ancelotti AC Jr. Thermal, rheological, and dielectric analyses of the polymerization reaction of a liquid thermoplastic resin for infusion manufacturing of composite materials. Polym Test. 2018;71:32-7. http://dx.doi.org/10.1016/j.polymertesting.2018.08.024.
56. Zoller A, Gigmes D, Guillaneuf Y. Simulation of radical polymerization of methyl methacrylate at room temperature using a tertiary amine/BPO initiating system. Polym Chem. 2015;6(31):5719-27. http://dx.doi.org/10.1039/C5PY00229J.
57. Vyazovkin S, Koga N, Schick C. Handbook of thermal analysis and calorimetry: recent advances, techniques, and applications. 2nd ed. Amsterdam: Elsevier; 2018. 842 p. (vol. 6).
58. Thiher NLK, Schissel SM, Jessop JLP. The influence of monomer chemistry on radical formation and secondary reactions during electron-beam polymerization. J Polym Sci. 2020;58(7):1011-21. http://dx.doi.org/10.1002/pol.20190113.
59. Botelho EC, Scherbakoff N, Rezende MC. Porosity control in glassy carbon by rheological study of the furfuryl resin. Carbon. 2001;39(1):45-52. http://dx.doi.org/10.1016/S0008-6223(00)00080-4.
60. Matyjaszewski K, Davis TP. Handbook of radical polymerization. Hoboken: John Wiley & Sons; 2002. 920 p. http://dx.doi.org/10.1002/0471220450.
61. Ma W, Yang G, Jiang K, Carpenter JH, Wu Y, Meng X, et al. Influence of processing parameters and molecular weight on the morphology and properties of high-performance PffBT4T-2OD:PC71 BM organic solar cells. Adv Energy Mater. 2015;5(23):1501400. http://dx.doi.org/10.1002/aenm.201501400.
62. Osswald TA, Menges G. Materials science of polymers for engineers. 3rd ed. Munich: Hnaser Publishers; 2010.

Materials Research. 2023; 26: e20210619er
DOI: https://doi.org/10.1590/1980-5373-MR-2021-0619er

Erratum: Kinetic and Viscoelastic Study of Liquid Thermoplastic Matrix Based on Methyl Methacrylate Copolymers

In the article "Kinetic and Viscoelastic Study of Liquid Thermoplastic Matrix Based on Methyl Methacrylate Copolymers", with DOI: https://doi.org/10.1590/1980-5373-MR-2021-0619, published in Materials Research, 26: e20210619, in the affiliations where it was written:

Daniel Consoli Silveira[a], Tiago Teixeira da Silva Braga[a], Luiza dos Santos Conejo[a,c],

Antônio Carlos Ancelotti Junior[b], Michelle Leali Costa[a,c], Edson Cocchieri Botelho[a]*

[a]Universidade Estadual Paulista, Departamento de Engenharia Civil, Guaratinguetá, SP, Brasil.
[b]Universidade Federal de Itajubá, Instituto de Engenharia Mecânica, Itajubá, MG, Brasil.
[c]Instituto de Pesquisas Tecnológicas, Laboratório de Estruturas Leves, São José dos Campos, SP, Brasil.

Should read:

Daniel Consoli Silveira[a], Tiago Teixeira da Silva Braga[a], Luiza dos Santos Conejo[a,c],

Antônio Carlos Ancelotti Junior[b], Michelle Leali Costa[a,c], Edson Cocchieri Botelho[a]*

[a]Universidade Estadual Paulista, Departamento de Materiais e Tecnologia, Guaratinguetá, SP, Brasil.
[b]Universidade Federal de Itajubá, Instituto de Engenharia Mecânica, Itajubá, MG, Brasil.
[c]Instituto de Pesquisas Tecnológicas, Laboratório de Estruturas Leves, São José dos Campos, SP, Brasil.

In the legend of figures 2 and 3, where it was written:

Figure 2. Heat flow vs. time curves for reactions with the autocatalytic mechanism of the polymeric systems.

Figure 3. Dynamic DSC of MMA systems and BzO initiator in different concentrations.

Should read:

Figure 2. Heat flow vs. time curves (exo up) for reactions with the autocatalytic mechanism of the polymeric systems.

Figure 3. Dynamic DSC of MMA systems and BzO initiator in different concentrations (exo up).